SOUND ATTENUATION IN FINITE - LENGTH SPLITTER SILENCERS

N. Sormaz (1), A. Cummings (1) and B. Nilsson (2).

(1) Department of Engineering Design and Manufacture, University of Hull, Hull, N. Humberside HU6 7RX.
(2) Fläkt Industri AB, Växjö, Sweden.

1. INTRODUCTION

In a previous paper, [1], the authors described a method for calculating the acoustic eigenvalues of an infinite-length splitter-type silencer. The theory was used to find all the eigenvalues which may exist in the silencer, without specifying the incident sound field, and measurements of attenuation and phase speed were taken for various modes which were excited by particular loudspeaker arrangements. If we assume that the incident sound field consists only of the fundamental mode, then, for a repetitive arrangement of baffles as described in [1], the only modes that are excited are those which occur in a 'half-module' as in Figure 1. This has been verified by using the present method to investigate a multi-splitter system. This theory may be used for an incident sound field consisting of any combination of propagating modes.

The authors sought a method for satisfying axial boundary conditions for different types of discontinuity. Existing methods include those of Miles [2] and Alfredson [3], who match the sound fields across discontinuities in rigid-walled ducts, but rely on the orthogonality of the eigensolutions and are valid only for low frequencies. Peat [4] uses weighting-functions to deal with area changes, incorporating mean flow; he also demonstrates the use of finite elements in modelling a discontinuity. Peat's method allows a system consisting of more than one discontinuity to be modelled, but assumes that only the plane wave propagates. It was decided here to use a variational approach which makes no assumptions of low frequency or orthogonality of the modes and allows the matching of sound fields in a bulk-reacting lining.

In this paper the method is demonstrated for modelling the end of a lined section of duct with a zero-thickness plate covering the end of the lining (Figure 1) and the results are compared to measurements taken on a test duct. Airflow has not yet been included in this model. This method is general and may be used for any duct discontinuity; results were obtained both with and without an end plate. The method has been used to predict values of transmission loss for a finite length lined section by treating both discontinuities (at each end of the lining) at the same time; comparisons with measured values are shown.

2. GEOMETRY

Figure 1 shows the model of this discontinuity. If the incident wave is plane, then the problem is two-dimensional, since no modes which vary in the z-direction will be excited. The incident wave is represented by p_I. p_A is the wave reflected from the termination and p_B is the transmitted wave in the lined section (it is assumed that p_B is not reflected from any discontinuity downstream); the suffices 1 and 2 distinguish

the eigenfunctions in the airway and liner. The widths of the airway and liner are a and h respectively. The lining may be anisotropic so two complex, frequency-dependent wavenumbers - k_a and k_l - and two complex, frequency-dependent densities - ρ_a and ρ_l - are needed to represent its bulk acoustic properties in the axial and transverse (x and y) directions respectively. The corresponding values in the airway are k and ρ_0; here, $k=\omega/c$, where ω is the radian frequency and c is the adiabatic sound speed in the air. Separate transverse coordinate systems, y_1 and y_2, are taken in the airway and liner.

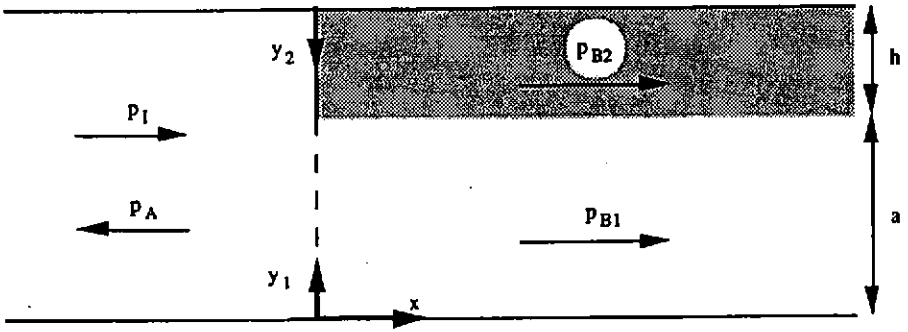

Figure 1 The discontinuity at the start of a lined section of duct.

3. THEORY

The pressure and particle displacement in the various regions may be written as

$$p_I(x,y_1;t) = P_0 \exp[i(\omega t - kx)] \quad (1a)$$

$$\xi_I(x,y_1;t) = \frac{-iP_0}{\rho_0 c^2 k} \exp[i(\omega t - kx)] \quad (1b)$$

$$p_A(x,y_1;t) = \sum_{j=1}^{\infty} a_j^* \cos p_j y_1 \exp[i(\omega t + \alpha_j^* x)] \quad (1c)$$

$$\xi_A(x,y_1;t) = \sum_{j=1}^{\infty} \frac{i a_j^* \alpha_j^*}{\rho_0 c^2 k^2} \cos p_j y_1 \exp[i(\omega t + \alpha_j^* x)] \quad (1d)$$

$$p_{B1}(x,y_1;t) = \sum_{j=1}^{\infty} b_j^* A_j \cos q_{j1} y_1 \exp[i(\omega t + \alpha_j^* x)] \quad (1e)$$

$$\xi_{B1}(x,y_1;t) = \sum_{j=1}^{\infty} \frac{-i b_j^* \beta_j^* A_j}{\rho_0 c^2 k^2} \cos q_{j1} y_1 \exp[i(\omega t + \alpha_j^* x)] \quad (1f)$$

$$p_{B2}(x,y_2;t) = \sum_{j=1}^{\infty} b_j^* \cos q_{j2} y_2 \exp[i(\omega t + \alpha_j^* x)] \quad (1g)$$

FINITE LENGTH SPLITTER SILENCERS

$$\xi_{B2}(x,y_2;t)=\sum_{j=1}^{\infty} \frac{-ib_j^*\beta_j^*}{\rho_a c^2 k^2} \cos q_{j2}y_2 \exp[i(\omega t+\alpha_j^* x)] \qquad (1h)$$

where P_0 is the amplitude of the incident wave, a_j^* and b_j^* are the unknown modal coefficients and α_j^* and β_j^* are the eigenvalues in the respective regions. The eigenfunctions in the lined section have been normalized at $y_2=0$. By setting y_2 as shown in Figure 1, the eigenfunctions may be written in the above simple form containing only a cosine function. The wavenumbers in the lined section are related in the following way, and may be found (and ordered) using the method described in [1] :

$$q_{j1}^2+\beta_j^{*2} = k^2 \qquad (2a)$$

$$q_{j2}^2+\beta_j^{*2} = k_a^2 \qquad (2b)$$

$$q_{j1}\rho_t \tan q_{j1}a = - q_{j2}\rho_0 \tan q_{j2}h \qquad (2c)$$

The reflected and transmitted modes originate from x=0 so it is required to non-dimensionalize the functions (1a-h) at that point

$$P_I= \exp[-i\omega t]\, p_I|_{x=0} /P_0= 1 \qquad (3a)$$

$$U_I=\frac{i\rho_0 c^2 k}{P_0} \exp[-i\omega t]\, \xi_I|_{x=0}= 1 \qquad (3b)$$

$$P_A= \exp[-i\omega t]\, p_A|_{x=0} /P_0=\sum_{j=1}^{\infty} a_j \cos p_j y_1 \qquad (3c)$$

$$U_A=\frac{i\rho_0 c^2 k}{P_0} \exp[-i\omega t]\, \xi_A|_{x=0} =\sum_{j=1}^{\infty} a_j \alpha_j \cos p_j y_1 \qquad (3d)$$

$$P_{B1}= \exp[-i\omega t]\, p_{B1}|_{x=0} /P_0 =\sum_{j=1}^{\infty} b_j A_j \cos q_{j1} y_1 \qquad (3e)$$

$$U_{B1}=\frac{i\rho_0 c^2 k}{P_0} \exp[-i\omega t]\, \xi_{B1}|_{x=0} =\sum_{j=1}^{\infty} b_j \beta_j A_j \cos q_{j1} y_1 \qquad (3f)$$

$$P_{B2}= \exp[-i\omega t]\, p_{B2}|_{x=0} /P_0 =\sum_{j=1}^{\infty} b_j \cos q_{j2} y_2 \qquad (3g)$$

$$U_{B2}=\frac{i\rho_0 c^2 k}{P_0} \exp[-i\omega t]\, \xi_{B2}|_{x=0} =\sum_{j=1}^{\infty} b_j \beta_j \rho_0/\rho_a \cos q_{j2} y_2 \qquad (3h)$$

The modal coefficients a_j^* and b_j^* are normalized by P_0 to a_j and b_j. The boundary conditions that are imposed on the discontinuities are

$$P_I(y_1)+P_A(y_1)=P_{B1}(y_1) \qquad 0\le y_1\le a \qquad (4a)$$

$$U_I(y_1)+U_A(y_1)=U_{B1}(y_1) \qquad 0\le y_1\le a \qquad (4b)$$

FINITE LENGTH SPLITTER SILENCERS

$$U_I(y_1)+U_A(y_1)=0 \qquad a\le y_1\le a+h \qquad (4c)$$

$$U_{B2}(y_2)=0 \qquad 0\le y_2\le h \qquad (4d)$$

These equations will be satisfied by a set of values of a_i and b_i which give a value of zero for the functional, I_n, where

$$I_n=\int_0^a [(P_I + P_A-P_{B1})\,\overline{(P_I +P_A-P_{B1})} + (U_I+U_A -U_{B1})\,\overline{(U_I+U_A-U_{B1})}]\,dy_1$$
$$+\int_a^{a+h} (U_I + U_A)\,\overline{(U_I+U_A)}\,dy_1 + \int_0^h U_{B2}\,\overline{U_{B2}}\,dy_2 \qquad (5)$$

The subscript, n, on I represents the number of modes on each side of the discontinuity that are used in the solution. The complex-conjugate of z is written as $\bar{z}$. If $z=x+iy$, then $z\bar{z}=x^2+y^2$, so this functional represents the sum of the squares of the differences in real and imaginary parts of the pressure and particle displacements across the discontinuity. The functional therefore depends quadratically on the real and imaginary parts of the modal coefficients (a_i^R, a_i^I, b_i^R and b_i^I). The superscripts R and I denote the real and imaginary parts of a variable. There is therefore one turning point, which, since the functional is positive for all a_i and b_i, must be a minimum. The values of a_i and b_i at this point represent the smallest error in the sound field across the discontinuity. The solution is found by minimizing the functional with respect to each of the a_i^R, a_i^I, b_i^R and b_i^I variables, i.e. differentiating with respect to each and setting the result to zero. It is convenient to write $\cos q_{i1}y_1$ and $\cos q_{i2}y_2$ as $f_1(y_1)$ and $f_2(y_2)$ and to split them into their real and imaginary parts, i.e.

$$f_{1i}^R(y_1) = \cos q_{i1}^R y_1 \cosh q_{i1}^I y_1$$
$$f_{1i}^I(y_1) = -\sin q_{i1}^R y_1 \sinh q_{i1}^I y_1$$
$$f_{2i}^R(y_2) = \cos q_{i2}^R y_2 \cosh q_{i2}^I y_2$$
$$f_{2i}^I(y_2) = -\sin q_{i2}^R y_2 \sinh q_{i2}^I y_2$$

A set of 4n equations, linear in the unknowns, is thus obtained, and may be written

$$\begin{bmatrix} XARAR & XARAI & XARBR & XARBI \\ XAIAR & XAIAI & XAIBR & XAIBI \\ XBRAR & XBRAI & XBRBR & XBRBI \\ XBIAR & XBIAI & XBIBR & XBIBI \end{bmatrix} \begin{bmatrix} a^R \\ a^I \\ b^R \\ b^I \end{bmatrix} = \begin{bmatrix} XAR \\ XAI \\ XBR \\ XBI \end{bmatrix}$$

where, for example, $XBRAI_{ij}$ represents the coefficient of a_j^I in the equation resulting from the functional being differentiated by b_i^R, and

$$XARAR_{ij} = XAIAI_{ij} = \int_0^a \cos p_i y_1 \cos p_j y_1\,dy_1 + (\alpha_i^R\alpha_j^R + \alpha_i^I\alpha_j^I)\int_0^{a+h} \cos p_i y_1 \cos p_j y_1\,dy_1$$

$$XARAI_{ij} = XAIAR_{ji} = (\alpha_i^I\alpha_j^R - \alpha_i^R\alpha_j^I)\int_0^{a+h} \cos p_i y_1 \cos p_j y_1\,dy_1$$

$$XARBR_{ij} = XBRAR_{ji} = XAIBI_{ij} = XBIAI_{ji} =$$
$$[A_j^R(\alpha_i^R\beta_j^R + \alpha_i^I\beta_j^I - 1) + A_j^I(\alpha_i^I\beta_j^R - \alpha_i^R\beta_j^I)] \int_0^a \cos p_i y_1\, f_{1j}^R(y_1)\,dy_1$$
$$-[A_j^I(\alpha_i^R\beta_j^R + \alpha_i^I\beta_j^I - 1) - A_j^R(\alpha_i^I\beta_j^R - \alpha_i^R\beta_j^I)] \int_0^a \cos p_i y_1\, f_{1j}^I(y_1)\,dy_1$$

FINITE LENGTH SPLITTER SILENCERS

$$XARBI_{ij} = XBIAR_{ji} = -XAIBR_{ij} = -XBRAI_{ji} =$$
$$[A_j^R(\alpha_i^I\beta_j^R - \alpha_i^R\beta_j^I) - A_j^I(\alpha_i^R\beta_j^R + \alpha_i^I\beta_j^I - 1)] \int_0^a \cos p_i y_1 \, f_{1j}^R(y_1)\, dy_1$$
$$- [A_j^R(\alpha_i^R\beta_j^R + \alpha_i^I\beta_j^I - 1) + A_j^I(\alpha_i^I\beta_j^R - \alpha_i^R\beta_j^I)] \int_0^a \cos p_i y_1 \, f_{1j}^I(y_1)\, dy_1$$

$$XBRBR_{ij} = XBIBI_{ij} = [(A_i^R A_j^R + A_i^I A_j^I)(1 + \beta_i^R\beta_j^R + \beta_i^I\beta_j^I) + (A_i^R A_j^I - A_i^I A_j^R)(\beta_i^I\beta_j^R - \beta_i^R\beta_j^I)]$$
$$\int_0^a \{f_{1i}^R(y_1) f_{1j}^R(y_1) + f_{1i}^I(y_1) f_{1j}^I(y_1)\}\, dy_1$$
$$+[(A_i^R A_j^I - A_i^I A_j^R)(1 + \beta_i^R\beta_j^R + \beta_i^I\beta_j^I) - (A_i^R A_j^R + A_i^I A_j^I)(\beta_i^I\beta_j^R - \beta_i^R\beta_j^I)]$$
$$\int_0^a \{f_{1i}^I(y_1) f_{1j}^R(y_1) - f_{1i}^R(y_1) f_1^R(y_1)\}\, dy_1$$
$$+ (\gamma_i^R\gamma_j^R + \gamma_i^I\gamma_j^I) \int_0^h \{f_{2i}^R(y_2) f_{2j}^R(y_2) + f_{2i}^I(y_2) f_{2j}^I(y_2)\}\, dy_2$$
$$+ (\gamma_i^R\gamma_j^I - \gamma_i^I\gamma_j^R) \int_0^h \{f_{2i}^I(y_2) f_{2j}^R(y_2) - f_{2i}^R(y_2) f_{2j}^I(y_2)\}\, dy_2$$

$$XBRBI_{ij} = XBIBR_{ji} = [(A_i^R A_j^R + A_i^I A_j^I)(\beta_i^I\beta_j^R - \beta_i^R\beta_j^I) - (A_i^R A_j^I - A_i^I A_j^R)(1 + \beta_i^R\beta_j^R + \beta_i^I\beta_j^I)]$$
$$\int_0^a \{f_{1i}^R(y_1) f_{1j}^R(y_1) + f_{1i}^I(y_1) f_{1j}^I(y_1)\}\, dy_1$$
$$+ [(A_i^R A_j^I - A_i^I A_j^R)(\beta_i^I\beta_j^R - \beta_i^R\beta_j^I) + (A_i^R A_j^R + A_i^I A_j^I)(1 + \beta_i^R\beta_j^R + \beta_i^I\beta_j^I)]$$
$$\int_0^a \{f_{1i}^I(y_1) f_{1j}^R(y_1) - f_{1i}^R(y_1) f_{1j}^R(y_1)\}\, dy_1$$
$$+ (\gamma_i^R\gamma_j^R + \gamma_i^I\gamma_j^I) \int_0^h \{f_{2i}^I(y_2) f_{2j}^R(y_2) - f_{2i}^R(y_2) f_{2j}^I(y_2)\}\, dy_2$$
$$- (\gamma_i^R\gamma_j^I - \gamma_i^I\gamma_j^R) \int_0^h \{f_{2i}^R(y_2) f_{2j}^R(y_2) + f_{2i}^I(y_2) f_{2j}^I(y_2)\}\, dy_2$$

$$XAR_i = \alpha_i^R \int_0^{a+h} \cos p_i y_1 \, dy_1 - \int_0^a \cos p_i y_1 \, dy_1$$
$$XAI_j = -\alpha_i^I \int_0^{a+h} \cos p_i y_1 \, dy_1$$
$$XBR_i = [A_i^R(1 + \beta_i^R) - A_i^I\beta_i^I] \int_0^a f_{1i}^R(y_1)\, dy_1 - [A_i^R\beta_i^I + A_i^I(1 + \beta_i^R)] \int_0^a f_{1i}^I(y_1)\, dy_1$$
$$XBI_i = -[A_i^R\beta_i^I + A_i^I(1 + \beta_i^R)] \int_0^a f_{1i}^R(y_1)\, dy_1 - [A_i^R(1 + \beta_i^R) - A_i^I\beta_i^I] \int_0^a f_{1i}^I(y_1)\, dy_1$$

The term $\gamma_j = \rho_0 \beta_j / \rho_a$ is introduced to simplify these expressions.The above set of equations may now be solved to find the modal coefficients which complete the solution of a semi-infinite lined duct. It may be shown that $I_n \geq I_{n+1}$, for all n; so the accuracy of a solution increases with increasing number of modes. The resulting value of the functional is an indicator to the accuracy of the solution.

A functional similar to (5), but with the extra boundary conditions at the downstream end of the lined section, has been used to predict values of transmission loss for a finite length of lined duct. The model takes all the modes into account at the downstream end, even though most of these will be strongly attenuated, and includes the reflection of these modes from the downstream termination.

The discontinuity without end-caps was treated in a similar manner, but the functional was changed so as to impose the boundary conditions of continuity of

pressure and particle displacement at the end of the lined section rather than setting the particle displacement to zero on either side of the end-plate ((4c) and (4d))

$$P_I(y_1)+P_A(y_1)=P_{B2}(a+h-y_1) \qquad a \le y_1 \le a+h$$

$$U_I(y_1)+U_A(y_1)=U_{B2}(a+h-y_1) \qquad a \le y_1 \le a+h$$

4. EXPERIMENTAL RESULTS

Measured data were taken in a test duct with cross-section 90mm by 100mm in which a plane incident wave was excited. Layers of fibre-glass of width 30mm were placed against both 100mm sides. Since a plane wave only excites even modes in a symmetric arrangement, this case is equivalent to that of Figure 1 with h=30mm and a=15mm. Tests were performed both with and without end plates.

Holes were drilled in one of the 90mm sides, 37mm from a corner, upstream and downstream of the discontinuity and measurements taken far enough in each direction so that the fundamental mode was the only mode present (in such a narrow duct the higher order modes will be highly attenuated in the frequency range considered). These measurements were then used to extrapolate back to the discontinuity and determine values of a_1. The value of b_1 was not found directly, but by extrapolation back to x=0 the value of $b_1 A_1 \cos(q_{11}$ 0.008) was calculated (y_1=8mm at the holes). This is because the fundamental reflected mode has constant amplitude across the duct, whilst the amplitude of the transmitted fundamental mode varies across the duct.

Figures 2(a,b) show comparisons of the magnitude and phase of the reflected wave relative to the incident wave, both with and without end-caps. Figures 3(a,b) show the same values for the transmitted fundamental mode. Agreement is good considering the possible loss of accuracy which may be introduced by the extrapolation and the excitation of higher order modes.

Transmission loss predictions are compared to measurements in Figures 4 and 5 and again agreement is good. For both figures, the lined section is 2m long and each end is covered by a plate. In Figure 4, h=150mm and a=75mm, whilst in Figure 5, h=150mm and a=150mm. The flow resistivity of the lining was 13800 Rayls/m in the transverse direction and was estimated to be 6900 Rayls/m in the axial direction; the bulk acoustic properties were found from the empirical formulae of Delany and Bazley [5]. The dashed line shows the attenuation of the least attenuated mode over the 2m length. For most of the frequency range there is no significant difference between the actual values and values for the least attenuated mode, however at both low and high frequencies the least attenuated mode prediction underestimates the transmission loss. The discrepancy at low frequencies is because the actual transmission loss is increased by more energy being reflected from the end-plate. It may be seen in Figure 3a that, at high frequencies, the magnitude of the fundamental mode is reduced; higher order modes are being excited to a greater extent and their decay rates are of the same order as the fundamental mode. The excitation of several modes to a lesser extent produces a transmission loss greater than that predicted on the basis of the least attenuated mode alone.

5. CONCLUSION

The variational method gives results that compare well with measured data, both for the single discontinuity and for predicting the transmission loss for a finite-length lined duct section. Numerical studies have been carried out on other discontinuities such as area-changes and diaphragms with mean flow; mean flow is to be incorporated into the model of the silencer.

6. REFERENCES

1. A. CUMMINGS and N. SORMAZ 1992 Journal of Sound and Vibration (to be published). Shorter version: 1991 Proceedings of the Institute of Acoustics 13, 443-452. Acoustic attenuation in dissipative splitter silencers containing mean fluid flow.

2. J.W. MILES 1946 The Journal of the Acoustical Society of America 17, 259-284. The analysis of plane discontinuities in cylindrical tubes.

3. R.J. ALFREDSON 1972 Journal of Sound and Vibration 23, 433-442. The propagation of sound in a circular duct of continuously varying cross- sectional area.

4. K.S. PEAT 1988 Journal of Sound and Vibration 127, 123-132. The acoustical impedance at discontinuities of ducts in the presence of a mean flow.

5. M.E. DELANY and N. BAZLEY 1970 Applied Acoustics 3, 105-116. Acoustical properties of fibrous absorbent materials.

7. ACKNOWLEDGEMENTS

The authors gratefully acknowledge Fläkt Industri AB, Växjö, Sweden, for supplying the experimental data in Figures 4 and 5, the Fraunhofer Institut für Bauphysik, Stuttgart, Germany, for permission to use the data, and support from the S.E.R.C. and Sound Attenuators of Colchester under Research Grant GR/F/59407.

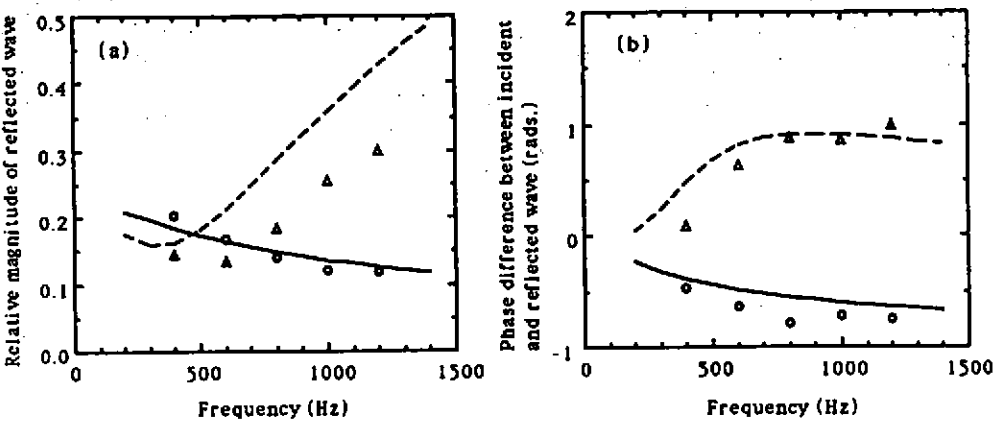

Figure 2. Relative magnitude (a) and phase difference (b) of the reflected fundamental mode, with end plates (▲, measured; ——, predicted) and without end plates (○, measured; – – –, predicted).

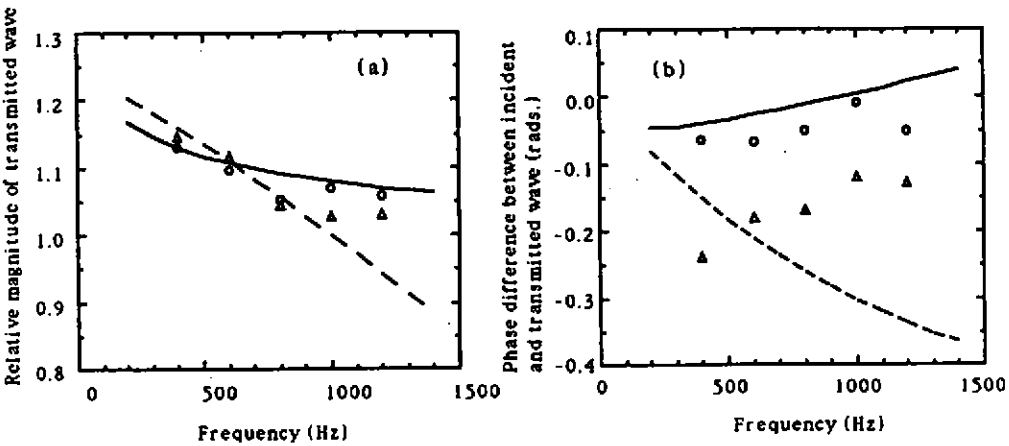

Figure 3. Relative magnitude (a) and phase difference (b) of the transmitted fundamental mode, with end plates (▲, measured; ——, predicted) and without end plates (○, measured; – – –, predicted).

FINITE LENGTH SPLITTER SILENCERS

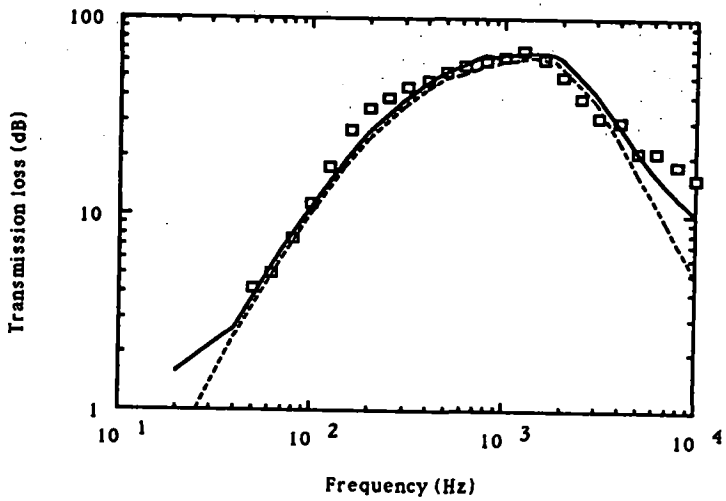

Figure 4. Transmission loss (measured, □ , and predicted, ——) and attenuation of least attenuated mode ,·----·, with h-0.15m, a-0.075m, l-2.0m.

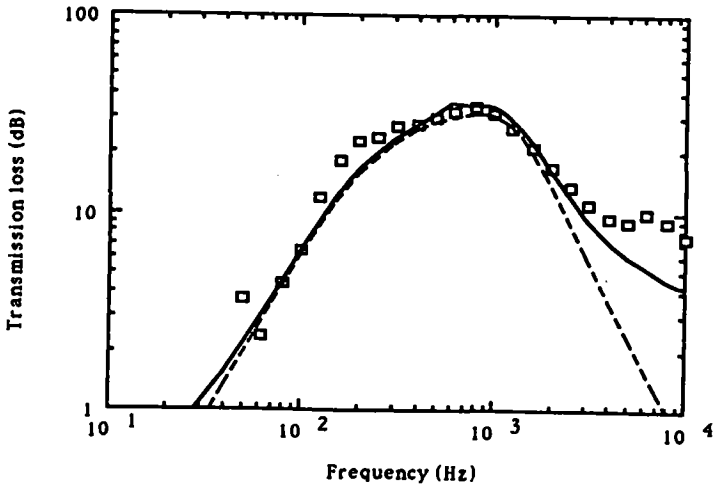

Figure 5. Transmission loss (measured, □ , and predicted, ——) and attenuation of least attenuated mode ,·----·, with h-0.15m, a-0.15m, l-2.0m.